

Electrical Measurements on Clean and Oxidized Germanium Surfaces*

Y. MARGONINSKI†

Raytheon Research Division, Waltham, Massachusetts

(Received 20 June 1963)

Simultaneous measurements of surface conductivity $\Delta\sigma$ and surface recombination velocity s were performed on 15 Ω -cm n -type germanium samples, cut perpendicular to the (111) or (100) axis. Clean surfaces were obtained by Farnsworth's technique of ion bombardment and anneal; the electrical measurements were performed with a Many bridge. The s of clean (111) surfaces varied between 730 cm/sec and 480 cm/sec and first decreased with oxygen adsorption. After an adsorption of about 300×10^{-6} Torr min, s started to increase and reached a value greater than that for the clean surface. The change of both s and $\Delta\sigma$ with oxygen adsorption depended strongly on the annealing temperature. The surface potential u_s of the clean surface was -9.9 ; i.e., strongly p -type but not degenerate. The s of the clean (100) surfaces varied between 320 cm/sec and 1040 cm/sec and changed very little with oxygen adsorption up to 50×10^{-6} Torr min, it then either decreased or continued to remain constant. The surface potential of the clean (100) surface was -14 ; i.e., degenerate p type. The field effect mobility of the clean (111) surface was $80 \text{ cm}^2 \text{ V}^{-1} \text{ sec}^{-1}$ and p type, that of the clean (100) surface $165 \text{ cm}^2 \text{ V}^{-1} \text{ sec}^{-1}$ (p type).

I. INTRODUCTION

COMBINED measurements of surface conductivity and recombination velocity have proved very successful in investigating the properties of real germanium surfaces. Such measurements have also been performed on clean surfaces^{1,2} but the results showed considerable disagreement and it was never found out whether this was due to a difference in cleaning procedures, sample resistivity, or crystal orientation. Reliable measurements of surface recombination alone has been carried out by Madden and Farnsworth³ and here again their results differ from those of Law and Garrett,² though both groups employed the ion-bombardment method for obtaining a clean surface. Surface conductivity (and field effect mobility) have been measured by many investigators and with much better agreement,⁴ though none of them succeeded in obtaining the surface potential of the clean surface.

In order to resolve some of the differences between these previous experimental results and to obtain additional information on clean surface parameters, combined measurements of surface conductivity and recombination velocity were performed on (111) and (100) germanium surfaces. Clean surfaces were obtained by Farnsworth's method of ion bombardment and anneal. As clean surfaces are known to be strongly p type, a special effort was made to create as strong a field as possible for the field effect measurements: for this reason the cleavage method⁵ for obtaining a clean surface had to be discarded. The electrical measurements were performed by employing the Many bridge

method⁶ rather than photoconductivity techniques for two reasons: (1) it is more sensitive and can detect inhomogeneity in surfaces ("patchiness"), and (2) for field effect measurements, and especially under ultra-high vacuum conditions, it appeared to require a less complicated experimental set up.

II. EXPERIMENTAL METHOD

1. Technique of Electrical Measurements

Simultaneous measurements of filament lifetime τ_f and conductivity $\Delta\sigma$ were performed with a Many bridge.⁶ This method requires one of the sample's contacts to be slightly injecting and the other to be ohmic. For this purpose soldered contacts are usually used. No soldered contacts could be used here because of their high vapor pressure at annealing temperatures, but it was found that gold plating the sample's edges resulted in slightly injecting and noise-free contacts which withstood well the repeated heat treatments. The diffusion of gold into germanium at annealing temperatures (550°C) is negligible. We were unsuccessful in finding satisfactory contacts for p -type material. As a detector for the Many bridge the Tetrax type 502 double beam oscilloscope was used; one beam for conductivity and the other for lifetime measurements. Changes in the sample's resistance of one part in 10 000 could be easily detected. The accuracy of the lifetime measurements depended on the injecting properties and varied between 2–15%. Dc voltages up to 1000 V were used for the field effect; the absence of slow states at pressures of 10^{-7} Torr and lower made ac voltages and phase shift arrangements⁷ unnecessary.

2. Crystal Mount and Field Plate Arrangement

The crystal mount and field plate arrangement are schematically illustrated in Fig. 1. The edges of the

* The research reported in this paper was sponsored by the U. S. Air Force Research Laboratories, Office of Aerospace Research, under contract AF 19(604)-8004.

† Present address: Department of Physics, Hebrew University, Jerusalem, Israel.

¹ S. Wang and G. Wallis, *J. Appl. Phys.* **30**, 285 (1959).

² J. T. Law and C. G. B. Garrett, *J. Appl. Phys.* **27**, 656 (1956).

³ H. H. Madden and H. E. Farnsworth, *Phys. Rev.* **112**, 793 (1958).

⁴ Y. Margoninski, *Ann. N. Y. Acad. Sci.* **101**, 915 (1963).

⁵ D. R. Palmer, S. R. Morrison, and C. E. Dauenbaugh, *J. Phys. Chem. Solids* **14**, 27 (1960).

⁶ A. Many, E. Harnik, and Y. Margoninski, in *Semiconductor Surface Physics*, edited by R. H. Kingston (University of Pennsylvania, Philadelphia, 1957), p. 85.

⁷ A. Many and D. Gerlich, *Phys. Rev.* **107**, 404 (1957).

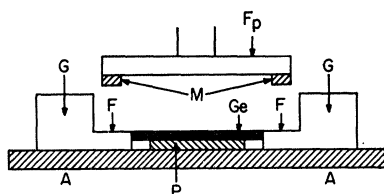


FIG. 1. Sample mount and field plate arrangement.

sample were pressed against two L-shaped graphite contacts G, one of them spring loaded. A precision ground quartz plate P was inserted between the sample and the base quartz plate A, so that the upper face of the sample was absolutely flush with the horizontal faces F of the graphite contacts. The field plate F_p , free to move in all directions, could be lowered until the 100- μ -thick mica spacers M rested firmly on the graphite faces F. In this manner a strong, homogeneous electric field was obtained and the danger of contaminating the cleaned surface with a dielectric spacer was avoided. During ion or electron bombardments the field plate was retracted into a side tube to prevent any sputtering onto the crystal face.

Figure 2 illustrates the main features of the experimental tube. The electron gun for ion bombardment, etc., was at about 10-cm distance from the field plate, so that after each cleaning operation the crystal had to be moved away from the electron gun and under the field plate. To accomplish this, the sample holder was mounted on a carriage which consisted of a nickel base B and two end plates H. The carriage could slide on the two tungsten rods R which passed through slots in the end plates H. The sliding movement was magnetically operated with the help of the nickel projections N which almost touched the inner wall of the glass tube. The tungsten rods R were held in position by a frame structure, consisting of two rails A_1 and A_2 and end rings D. The upper rail A_1 had two large slots, one for the electron gun and the other, not shown in Fig. 2, for the field plate. The metal tongues L pressed against the inner wall of the glass tube and the entire frame could be centered and positioned by adjusting screws, not shown in the figure. The two end rings D on each side of the frame also supported short glass tubes, through which passed the electrical connections (tungsten coils) to the graphite contacts. Not shown in Fig. 2 are quartz plates which covered the vertical faces of the contacts and prevented graphite from sputtering onto the

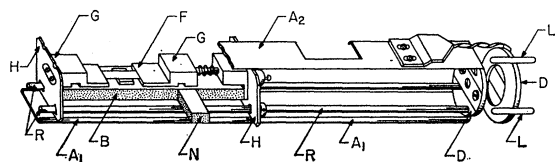


FIG. 2. Sketch of the experimental tube.

crystal face, and mica spacers which insulated the contacts from the end plates H.

Figure 3 is an illustration of the field plate. The plate itself F_p was made from a H-shaped nickel block, the lower part precision machined to ensure absolute flatness. The nickel block was attached to a bar B (of square cross section) by two screws S, resting on the plate P. In this manner the nickel block had small freedom of movement in every direction and could easily "find its position" when lowered onto the graphite contacts. The frame, which held the bar B in position inside the vertical side tube, utilized a "clock construction." In the lowered position the nickel slug A (for the magnetic control) rested on the set screw R. To remove the field plate from the crystal mount, A was lifted and rotated until it rested on the set screw C.

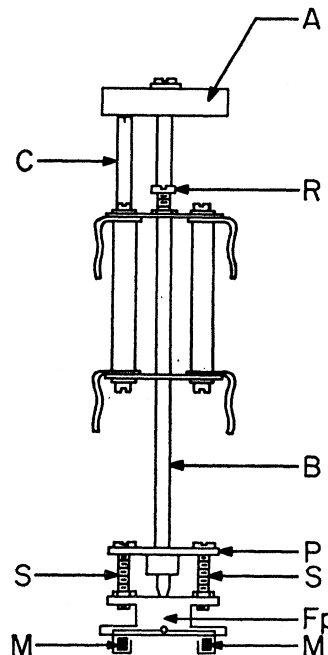


FIG. 3. Sketch of the field plate.

The two mica spacers M were attached to the field plate by two tungsten hooks.

During the first field-effect measurements it was found that the field plate was very often "shortened" by small graphite or metal particles on the contacts. The thickness of the mica spacers was therefore increased from 40 to 100 μ and this prevented the occurrence of "shorts" in most cases. The capacity of the sample-field plate capacitor was 9 $\mu\mu$ F.

3. Vacuum System

The ultrahigh vacuum system is illustrated in a block diagram, Fig. 4. The main system and the gas handling system were pumped by a forepump and a single-stage mercury diffusion pump to about 5×10^{-7} Torr. The ultrahigh vacuum part of the system could be baked

out at 280°C. This is the part above the dashed line in Fig. 4. It contained an omegatron mass spectrometer of the type described by Zdanuk *et al.*,⁸ a "Varian type V-11403" vacuum ion pump (pumping speed: 5 liter/sec), a "N.R.C. model 552" Redhead magnetron gauge, a "Westinghouse WL5966" B-A ion gauge, and a "Wolsky type 3" molybdenum getter. The lowest pressures ($\sim 7 \times 10^{-10}$ Torr) were obtained immediately after bakeout; after the bombardment and annealing processes it increased from about 8×10^{-9} to 2×10^{-8} Torr. Residual gas scans were carried out after each operation as a routine procedure. During the adsorption runs a steady flow of oxygen was passed through the system at 2 liters/sec and a pressure of about 5×10^{-6} Torr was maintained and measured with the help of the Redhead magnetron gauge, which does not cause any CO₂ and CO conversion.⁹

4. Crystal Preparation and Surface Cleaning

All samples were cut from a 15 Ω -cm *n*-type single crystal obtained from Semimetals, Inc. of Long Island, New York. From this crystal the first slices were cut parallel to the 111 face. (This was the direction in which the crystal was grown.) It was then reoriented by Laue x-ray back reflections, so that slices could be cut parallel to the 100 face. From these slices, 0.4-cm-wide rectangular strips were cut and ground down to a thickness of 0.05 cm. Resistivity scans were then performed to test if the doping was homogeneous throughout the length of the strip and 2-cm-long samples were cut off each strip accordingly. The edges of each sample were then gold plated. To ensure that only those parts of the crystal remained gold plated that actually touched the L-shaped graphite contacts (Fig. 1), the sample was ground down to a thickness of 0.045 cm and width of 0.39 cm. The final shape of the sample, prior to etching, was that of a parallelepiped with dimensions $2 \times 0.39 \times 0.045$ cm. The gold-plated edges were masked and the sample etched in CP-4A for one minute at 35°C, it was then stored in room air for a few days. The reason for this etching and storage in room air was because this is one of the standard treatments for real surfaces and some samples were measured under ordinary vacuum conditions, to investigate their surface state parameters prior to ion and electron bombardment.

The cleaning procedure closely followed the ion-bombardment technique of Madden and Farnsworth.³ The sample was argon bombarded for 40 min at a pressure of $(3-8)10^{-8}$ Torr, using a controlled discharge produced by electron beams of 60–80 eV. The current density was 200–800 $\mu\text{A}/\text{cm}^2$ and the bombarding voltages were 500–800 V. The argon was pumped out and the crystal annealed, by electron bombardment, to about 550°C for 15 h. By slowly reducing the high

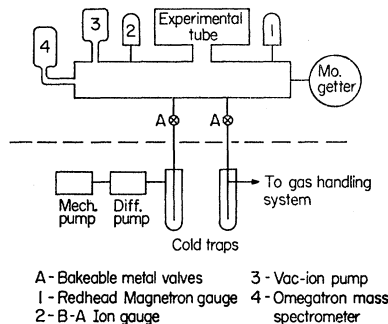


FIG. 4. Block diagram of the ultra-high vacuum system.

voltage the sample was cooled down to room temperature in about 5 h. During the ion bombardment the metal frame of the experimental tube (Fig. 2) was connected to the accelerating grid of the electron gun. During electron bombardment the frame was grounded. The annealing temperature of the sample was obtained by calibrating the bombarding electron current against a thermocouple attached to the crystal. The thermocouple wires were removed after the calibration curve had been obtained. To heat the crystal to 550°C, about 15 W were required (2000 V, 7–8 mA), but a substantial part of this power was wasted on the graphite contacts.

The mica spacers (Figs. 1 and 3) insulating the graphite contacts from the field plate were originally clamped to these contacts. However, it was noticed that under electron bombardment the mica would start to glow brightly at certain spots and burn away at the edges. This would cause the pressure to rise from 10^{-7} to 10^{-5} Torr. The mica spacers were then attached to the field plate, and this increased the crystal's temperature considerably (for the same electron current) and decreased the gas pressure during electron bombardment by two orders of magnitude.

III. EXPERIMENTAL RESULTS

1. Interpretation of Data

The measured quantities were filament lifetime τ_f and filament resistance R_f , these had to be converted into surface recombination velocity s and surface conductivity $\Delta\sigma$. In calculating the values of s and $\Delta\sigma$ corrections had to be applied to take into account that only one of the two large sample surfaces was ion bombarded and therefore atomically clean. Values of $\Delta\sigma$ were corrected by a method similar to that used by Forman¹⁰: Preliminary oxygen adsorption experiments were performed on samples which were subjected to electron bombardment only. From these measurements the influence of the surface not exposed to argon bombardment could be determined. As will be shown in paragraph 3 of this section, the unbombarded surface changed relatively little with oxygen adsorption and therefore acted like a parallel resistor of almost constant value.

⁸ E. J. Zdanuk, R. Bierig, L. G. Rubin, and S. P. Wolsky, *Vacuum* **10**, 382 (1960).

⁹ R. E. Schlier, *J. Appl. Phys.* **29**, 1162 (1958).

¹⁰ R. Forman, *Phys. Rev.* **117**, 698 (1960).

The surface recombination velocity s was corrected by employing¹¹:

$$\frac{1}{\tau_f} = \frac{1}{\tau_b} + \frac{s_1}{B} + \frac{s_2}{B}, \quad (1)$$

where τ_b, τ_f = bulk and filament lifetime, B = half the sample thickness, and s_1, s_2 are the surface recombination velocities of the two large sample surfaces. Equation (1) applies only for small values of s , i.e., as long as $\eta = tg\eta$.¹¹ This condition was fulfilled in almost all cases. It should also be remembered that for the interpretation of our data the changes in s are far more important than their absolute values.

2. (111) Surfaces

All together three samples of (111) orientation were investigated. Each was subjected to four or five oxygen adsorption experiments. Very similar results were obtained on all three samples.

The surface recombination velocity s of the first sample (Se1|6|1) in room air was 190 cm/sec, at 10^{-4} Torr; s was 360 cm/sec, and after bakeout and at 1×10^{-8} Torr it increased to 550 cm/sec. This progressive increase was also observed by Madden and Farnsworth,³ and is due to the removal of water vapor from the sample.¹² For the different adsorption runs, the recombination velocity for the clean surface varied between 730 cm/sec and 480 cm/sec. Madden³ quotes a value of 460 cm/sec and Law and Garrett² measured 600 cm/sec on their p -type sample. However, when oxygen was admitted to the system results were obtained which differed significantly from those reported earlier.^{2,3} The results of two different oxygen adsorption runs are represented in Fig. 5, which illustrates the changes in s and $\Delta\sigma$ as a function of the product (pressure \times time). Changes in $\Delta\sigma$ are relative to an arbitrary zero before oxygen admission. All in all five

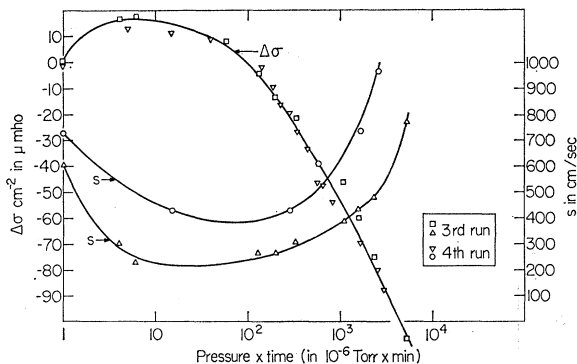


FIG. 5. s and $\Delta\sigma$ as functions of oxygen adsorption, (111) surface.

¹¹ W. Shockley, *Electrons and Holes in Semiconductors* (D. Van Nostrand, Inc., New York, 1950), p. 318.

¹² Y. Margoninski and H. E. Farnsworth, *Phys. Rev.* **123**, 135 (1961).

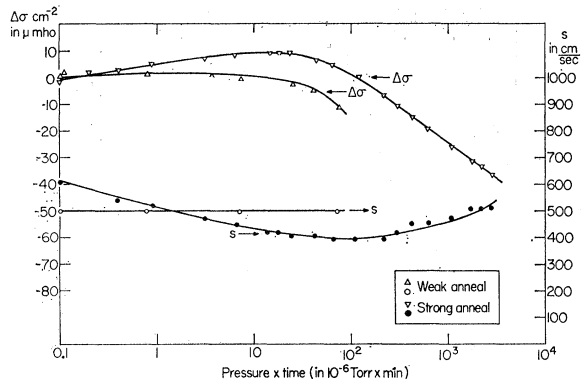


FIG. 6. s and $\Delta\sigma$ as functions of oxygen adsorption for different annealing temperatures, (111) surface.

adsorption experiments were performed on this first sample. For the first three runs the surface was cleaned by ion bombardment and annealing, but for the last two it was cleaned by annealing only. Figure 5 gives the results for the third and fourth adsorption runs. It is clearly seen that in both cases the surface recombination velocity first decreased and then, after about 300×10^{-6} Torr min, started to increase and reached a value greater than that for the clean surface. Exactly the same behavior was observed on all adsorptions. After five consecutive runs on the first sample, four additional experiments were performed on a second sample (Se1|5|3). Here again very similar results were obtained; s first decreased and then increased with oxygen adsorption. Following the third adsorption, the sample was heated to 130°C at 3×10^{-6} Torr oxygen pressure for over 15 h, but this additional treatment decreased s by only 10%. The changes in $\Delta\sigma$ with oxygen adsorption reported here agree very well with those previously observed by Law and Garrett² and Palmer *et al.*⁵ Decrease of s with oxygen adsorption has never been observed before and it was thought that insufficient annealing after ion bombardment may have been the reason. The third sample (Se1|4|3) was therefore annealed at temperatures lower than 550°C , before being exposed to oxygen. Figure 6 illustrates the results of two consecutive adsorptions, differing only in their annealing temperature. When this temperature was below 500°C , no change in s was observed and the initial increase of $\Delta\sigma$ was small, but after reannealing at 550°C the usual changes in s and $\Delta\sigma$ were observed. During another adsorption performed after insufficient annealing no initial change in s was detected, but after 10^{-3} Torr min the surface recombination started to increase. In other words, results similar to those published by Madden³ and Law² could be obtained by decreasing the annealing temperature. {It is interesting to point out that F. G. Allen and G. W. Gobeli [Bull. Am. Phys. Soc. **8**, 297 (1963)] reported considerable changes in work function and photoelectric yield on cleaved silicon surfaces upon annealing.} It should however be

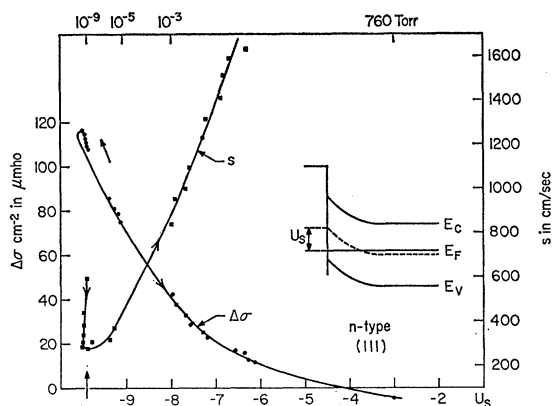


FIG. 7. s and $\Delta\sigma$ as functions of surface potential, (111) surface.

mentioned that in most cases the injecting properties of the gold-plated contacts improved with increased temperature. The accuracy and sensitivity of the lifetime measurements performed after insufficient annealing were therefore noticeably inferior to those preceded by higher annealing temperatures. Moreover, Madden⁸ measured surfaces parallel to the (100) direction and here his results are in good agreement with ours, as will be seen later. The third sample, after completion of an oxygen adsorption run, was exposed to the atmosphere. Field effect measurements then showed that the minimum of $\Delta\sigma$ could be reached. It was therefore possible to measure $\Delta\sigma$ in absolute units and thereby determine the surface potential¹³ $u_s = q\phi_s/kT$ throughout the entire range, starting with the clean surface at 10^{-8} Torr and terminating with the real surface at 760 Torr. The results are shown in Fig. 7, which also illustrates the energy level diagram of the clean (111) surface. E_V = top of valence band, E_C = bottom of conduction band, E_F = Fermi level, the intrinsic level E_i is indicated by the dashed line. The pressure scale in Fig. 7 is only approximate. The surface potential of the clean surface was $u_s = -9.9$. After 14×10^{-6} Torr min it reached -10 and from thereon decreased continuously with oxygen adsorption. At atmospheric pressure $u_s = -3$, the minimum of $\Delta\sigma$ extended from (-1) to (-3) . These results therefore indicate that the clean (111) surface is highly p type, but *not* degenerate.

The field effect mobility of the clean surface of sample Se1|5|3 was $80 \text{ cm}^2 \text{ V}^{-1} \text{ sec}^{-1}$ and p type, in excellent agreement with the values $(50-150) \text{ cm}^2 \text{ V}^{-1} \text{ sec}^{-1}$ quoted by Palmer *et al.*⁵ After oxygen adsorption of 450×10^{-6} Torr min the mobility was $88 \text{ cm}^2 \text{ V}^{-1} \text{ sec}^{-1}$ and p type, i.e., it had hardly changed. Handler¹⁴ and Forman¹⁰ also reported that the field effect mobility remained almost

constant during the initial phases of oxygen adsorption. The mobility of sample Se1|4|3 at 10^{-6} Torr, and before the cleaning process was $90 \text{ cm}^2 \text{ V}^{-1} \text{ sec}^{-1}$ and n type; after the system was baked out and the pressure decreased to 5×10^{-9} Torr the sample's mobility reached $200 \text{ cm}^2 \text{ V}^{-1} \text{ sec}^{-1}$ (n type).

3. (100) Surfaces

Two samples of (100) orientation were investigated, the first (Se1|100|3|2) was subjected to four oxygen adsorption runs, the second sample (Se1|100|2|1) to three runs. Because of the poorer injecting qualities of the contacts only two out of the seven adsorption runs permitted accurate measurements of filament lifetime; surface conductivity measurements were not adversely affected by this.

Figure 8 illustrates the results obtained on a non-ion bombarded surface, after annealing and exposure to oxygen, (Sample Se1|100|2|1). $\Delta\sigma$ changed very little with oxygen adsorption on these "unclean" surfaces, s remained constant up to 40×10^{-6} Torr min and then increased slowly. The entire change in filament lifetime τ_f during this experiment was from $44 \mu\text{sec}$ (at 8×10^{-9} Torr) to $33 \mu\text{sec}$ (2×10^{-8} Torr min) and the accuracy was very satisfactory. After subsequent ion bombardment and anneal the results represented in Fig. 9 were obtained. The changes in $\Delta\sigma$ are very similar in character to those on (111) surfaces (Fig. 5), but much faster. The filament lifetime changed very little throughout the entire experiment, from 11.5 to $12.5 \mu\text{sec}$ and unfortunately the accuracy was extremely poor. The surface recombination velocity of the clean surface, obtained from τ_f and the s values of the nonbombarded surface (Fig. 8) with the help of Eq. (1), exhibits a rather sharp decrease after about 10^{-4} Torr min. This is due to the fact that s of the nonbombarded surface *increases* slightly in this region (Fig. 8) whereas the bombarded surfaces exhibit a small *decrease* in s (points marked "measured values of s " in Fig. 9). The "corrected values of s " (Fig. 9) are therefore equal to the difference between two magnitudes changing slowly in

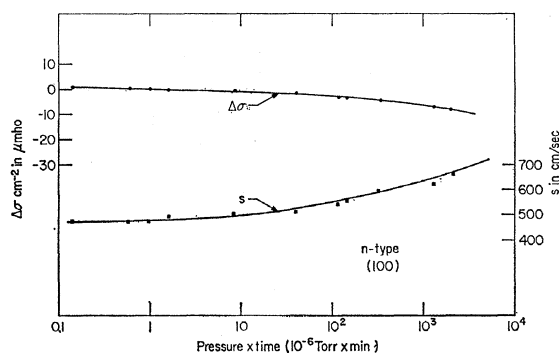


FIG. 8. s and $\Delta\sigma$ during oxygen adsorption on non-ion bombarded (100) surfaces.

¹³ R. H. Kingston and R. F. Neustadter, J. Appl. Phys. **26**, 718 (1955).

¹⁴ P. Handler and W. M. Portnoy, Phys. Rev. **116**, 516 (1960).

opposite directions, B/τ_f and s_1 , and change therefore much faster than either of them. Because of the poor experimental accuracy in τ_f the results of Fig. 9 should only be interpreted as indicating little or no change in s up to about 10^{-4} Torr min, this was also confirmed by all the other adsorption experiments performed on (100) surfaces. After exposing Se1|100|2|1 to air the minimum of $\Delta\sigma$ could be reached and the surface potential u_s was determined. The results are shown in Fig. 10, which also illustrates the energy level diagram of the clean (100) surface. The surface potential of the clean surface was -13.9 ; the surface was therefore p type and degenerate. Forman¹⁰ also found that the (100) surface was more p type than the (111) surface, but did not quote any values. It is interesting to note that the results of Fig. 9 cover only a span from $u_s = -14$ to about $u_s = -12.3$; i.e., the region of a degenerated surface. Values of field-effect mobility measured on sample Se1|100|3|2 were as follows:

At 5×10^{-9} Torr, before argon bombardment:	470 $\text{cm}^2 \text{V}^{-1} \text{sec}^{-1}$ (n type)
After argon bombardment:	35 $\text{cm}^2 \text{V}^{-1} \text{sec}^{-1}$ (n type)
Clean surface:	165 $\text{cm}^2 \text{V}^{-1} \text{sec}^{-1}$ (p type)
After oxygen adsorption, at 10^{-5} Torr oxygen pressure:	180 $\text{cm}^2 \text{V}^{-1} \text{sec}^{-1}$ (p type)
After exposure to atmosphere:	140 $\text{cm}^2 \text{V}^{-1} \text{sec}^{-1}$ (p type).

The extreme low value of the mobility after argon bombardment is remarkable, similar results were also obtained by Forman.¹⁰ After exposure to the atmosphere the surface conductivity was very near its minimum, which explains the low value of $140 \text{ cm}^2 \text{V}^{-1} \text{sec}^{-1}$.

After their removal from the experimental tube most samples of either (100) or (111) orientation were subjected to field effect measurements, utilizing two field plates and mica spacers⁶ to investigate their surface states. All these attempts were unsuccessful because the applied fields were insufficient to pass over the plateau region of maximum s .

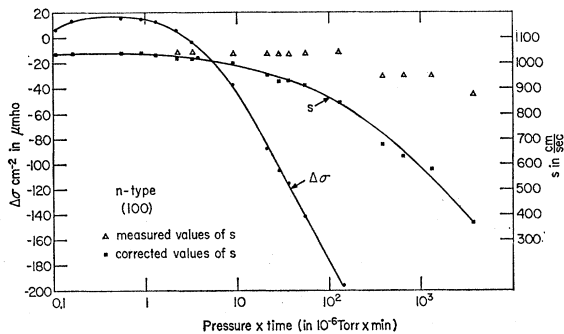


FIG. 9. s and $\Delta\sigma$ during adsorption, (100) surfaces.

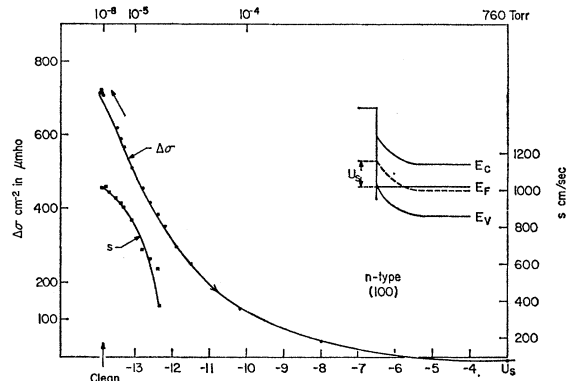


FIG. 10. s and $\Delta\sigma$ as functions of surface potential, (100) surface.

4. Slow States Relaxation Effects

It was inevitably observed on all samples that the slow states relaxation effects (of s and $\Delta\sigma$) disappeared after the vacuum system had been baked out and a pressure of 5×10^{-9} Torr obtained. The same observation has been reported by Palmer *et al.*⁵ and by others.¹⁵ To shed some additional light on this subject, the following sequel of experiments was performed: Sample Se1|4|3 was etched in CP-4A and stored in room air for a few days. It was then introduced into an ordinary vacuum system and the relaxation effects of s and $\Delta\sigma$ were measured at 2×10^{-5} Torr. These effects were of exactly the same nature as those reported by Many *et al.*¹⁶ The sample was removed and introduced into the ultrahigh vacuum system, where it was subjected to ion bombardment, electron bombardment, and oxygen adsorption experiments. After the completion of the fifth adsorption run the sample was exposed to the atmosphere and tested for relaxation effects. At atmospheric pressure these effects were present. When evacuated to 2×10^{-5} Torr no effects whatsoever could be observed, though fields of $1 \times 10^6 \text{ V/cm}$ were applied for 5 min and resistance changes of 0.02% could have been detected. This proves that the relaxation effects observed under ordinary vacuum conditions are not caused by any ad- or desorption of ions from the surrounding ambient, as was assumed by Low¹⁷ and by Lyashenko *et al.*¹⁸ In fact, these relaxations are not related at all to the ambient but inherent in the oxide structure that covers the germanium surface. The slow states are probably very closely connected with water molecules in the

¹⁵ M. Lax, in *Proceedings of the International Conference on Semiconductor Physics, 1960* (Academic Press Inc., New York, 1961), p. 484.

¹⁶ A. Many, Y. Margoninski, E. Harnik, and E. Alexander, *Phys. Rev.* **101**, 1433 (1956).

¹⁷ G. E. Low, *Proc. Phys. Soc. (London)* **B68**, 10 (1955).

¹⁸ V. I. Lyashenko and N. S. Chernaya, *Fiz. Tverd. Tela* **1**, 799, 921 (1959) [translations: *Soviet Phys.—Solid State* **1**, 799, 921 (1959)].

TABLE I. Residual gas scans (%).

No.	Conditions	Ions Mass number >44	CO ₂ ⁺ 44	Ar ⁺ 40	O ₂ ⁺ 32	N ₂ ⁺ CO ⁺ 28	Ar ⁺⁺ 20	H ₂ O ⁺ 18	OH ⁺ 17	CH ₄ ⁺ O ⁺ 16	(CO) ⁺⁺ N ⁺ 14	C ⁺ 12	Total pressure (Torr)
1	Before bakeout	52				5		43					2×10 ⁻⁴
2	After system was baked out	1	28			48		14	4.6	2.5		2.6	8×10 ⁻⁸
3	Electron gun outgassing	0.7	8.8	1.7		76		4.8	1.5	1.7	0.7	1.2	1×10 ⁻⁶
4	After argon bombardment	3	24	19		34	1	12	4.6	1.7		...	3×10 ⁻⁸
5	Crystal heated by electron bombardment	10	7.6	53		17	2.3	6	2.3	1.5		...	2×10 ⁻⁷
6	During oxygen adsorption	...	7.4	3	76.5	3		10					1×10 ⁻⁵
7	After oxygen adsorption		26	11.3	20	25	1.4	9	3	4	0.8		2×10 ⁻⁷
8	After flashing getter	1.3	25	22	7	15	1.3	17	7.6	3	1		5×10 ⁻⁸

oxide structure,¹⁹ because the germanium oxide covering the clean surface was formed with no traces of water vapor present, and indeed did not show any relaxation phenomena. Relaxations at *atmospheric pressure* may be due to ad- or desorption of ions, but are probably caused by the water vapor in the atmosphere.

5. Residual Gas Analysis

Table I summarizes the main features of residual gas scans during various stages of the research. The results are quoted in percentage of total pressure and therefore indicate directly the composition of the residual gas. The following features are noteworthy: (1) The percentage of oxygen (mass number 32 and 16) at pressures below 8×10⁻⁸ never exceeds 10%. (2) Argon, once admitted to the system, is persistently present and its percentage increases the lower the total pressure. It is also mainly responsible for the pressure rise during electron bombardment and does not disappear, even after prolonged heating. Argon ions, even at such low energies as 600–800 eV, seem to penetrate quite deeply into the crystal²⁰ and into the graphite contacts. (3) The very small oxygen conversion effect⁹ of the well decarbonized omegatron filament should be noted (scan No. 6). (4) The efficiency of the getter in pumping oxygen is well illustrated by comparing scans No. 7 and No. 8.

These results are similar to those reported by Wolsky and Zdanuk.²¹ Three mass numbers higher than 44 were consistently encountered: 200, 110, and 70. Mass number 200 was most probably due to Hg⁺ and 110 might have been Hg⁺⁺, but the origin of mass number 70 remained a mystery. The obvious suggestion would be Ge⁺ (mass number 72.6) but the following two facts almost rule it out: (1) The distance between the sample and the omegatron was about 40 cm and no traces of

Ge could possibly reach the omegatron. (2) The mass number 70 peak was not increased when the sample was heated by electron bombardment. The resolution of the omegatron for these high mass numbers is poor and for this reason no satisfactory evidence for either GeO⁺ or GeO₂⁺ could be found.

IV. CONCLUSIONS AND DISCUSSION

The results reported here indicate that the clean (111) germanium surface is strongly *p* type, but not degenerate and the valence band is at a distance of about $q\phi_s = 4kT$ below the Fermi level. The surface recombination is not space charge limited and is noticeably affected by oxygen. The changes in $\Delta\sigma$ and s after admitting oxygen to the clean surface (Figs. 6 and 8) can most simply be explained²² by assuming the surface to become even more *p* type during the initial phases of oxygen adsorption, up to about a monolayer or so, followed by a continuous decrease of the surface potential towards the "flat band" configuration. This would also account for the rise in work function observed by Dillon and Farnsworth²³ on (111) and (100) surfaces. In calculating the values of u_s from the experimental results of $\Delta\sigma$ no "Schrieffer corrections"²⁴ were applied and the bulk values of the mobilities were used. Lacking reliable experimental confirmation of Schrieffer's correction for strongly *p*-type surfaces, this seemed the most sensible thing to do. This uncertainty for the hole mobility at the clean surface will cause some error in the value $u_s = -9.9$ of the surface potential, but it can hardly be greater than (∓ 1), because of the steepness of the $\Delta\sigma(u_s)$ curve in this region. Kingston and Neustadter's plot of the $G(u_s, u_b)$ functions¹³ could not be used because they do not cover the range of u_s values needed here, so the corresponding curves published by Many *et al.*²⁵ were used. (The

¹⁹ M. Lasser, C. Wysocki, and B. Berstein, in *Semiconductor Surface Physics*, edited by R. H. Kingston (University of Pennsylvania, Philadelphia, 1957), p. 147.

²⁰ E. V. Kornelsen, Twenty Third Annual Conference on Physical Electronics, MIT, Cambridge, Massachusetts, 1963 (unpublished).

²¹ S. P. Wolsky and E. J. Zdanuk, *J. Phys. Chem. Solids* **14**, 124 (1960).

²² P. Handler, in *Semiconductor Surface Physics*, edited by R. H. Kingston (University of Pennsylvania, Philadelphia, 1957), p. 23.

²³ J. A. Dillon and H. E. Farnsworth, *J. Appl. Phys.* **28**, 174 (1957).

²⁴ J. R. Schrieffer, *Phys. Rev.* **97**, 641 (1955).

²⁵ A. Many, N. B. Grover, and Y. Goldstein, in *Semiconductor Surfaces* [North-Holland Publishing Company, Amsterdam (to be published)].

author would like to thank Dr. N. Grover for making these curves available to him, prior to their publication.)

Palmer *et al.*²⁶ reported a value of $0.33 \text{ eV} = -12.5 kT$ for their cleaved (111) surface (measured on a *p-n-p* transistor-like structure of $7 \Omega\text{-cm}$ resistivity) i.e., the Fermi level at the surface was near the edge of the valence band. This indicates a *p*-type degenerate surface; however, recent results obtained at the Bell Telephone Laboratories²⁷ showed that the clean germanium surface was *not* degenerate.

The cleaned (100) surface is *p* type, degenerate, and the valence band touches the Fermi level. Madden's³ previous findings were confirmed and the surface recombination is almost unaffected up to an oxygen adsorption of about 10^{-4} Torr min. This can be explained by assuming the recombination to be space charge limited,²⁸ i.e., the strong *p*-type barrier prevents the electrons from reaching the surface. The surface recombination seemed to remain unaffected for even more prolonged periods of oxygen adsorption, but the experimental evidence here is less reliable and more data are needed. The remark made previously on the possible error in the value of u_s for the clean (111) surface applies even more to the value of $u_s = -13.9$ for the (100) surface. In fact, this value should be regarded as a lower limit; i.e., our results indicated that the surface potential of the clean (100) surface was *at least* -13.9 .

Dillon and Farnsworth²⁸ measured the work function and photoelectric threshold of a (110) surface, $42 \Omega\text{cm}$ material, and reported the values of 4.78 eV and 4.68 eV, respectively. Their surface was therefore highly *p*-type degenerate. Assuming no electron emission from surface states,²⁹ the corresponding u_s value would be about -18 . This is much higher than any value measured by surface conductivity. Moreover, the (110) surface has the same number of free bonds per surface atom as the (111) surface and one would expect the surface potential of the (110) surface to be close to that of the (111) orientation. There is little doubt that Dillon and Farnsworth's value of $q\phi_s = -18 kT$ is at least as accurate as any value based on surface conductivity measurements. Perhaps here is an indication that the hole mobility at a clean germanium surface is reduced far more than one had expected: Assuming the hole mobility to be equal to its bulk value, the surface conductivity for $u_s = -18$ is about $9000 \mu\text{mho cm}^{-2}$. The highest value of $\Delta\sigma$ we measured [on a (100) surface] was $720 \mu\text{mho cm}^{-2}$, so this would point to a twelve-fold reduction in mobility. Unfortunately, Dillon and Farnsworth²⁸ measured the photoelectric threshold only for (110) surfaces and a similar com-

parison for other surface orientations can therefore not be made.

From the values of the field effect mobility an estimate on the density of the surface states can be obtained. For the nondegenerate (111) surface the following formula applies²⁸:

$$\left| \frac{\mu_{FE}}{\mu} \right| = \frac{1}{1 + S_E \times 2kT/\Delta P}, \quad (2)$$

where μ_{FE} = field effect mobility, μ = hole mobility, ΔP = surplus concentration of holes,¹³ and S_E = density of surface states per $\text{cm}^2 \times \text{eV}$.

For the clean (111) surface: $\mu_{FE} = 80 \text{ cm}^2 \text{ V}^{-1} \text{ sec}^{-1}$, and $\Delta P = 5 \times 10^{11} \text{ cm}^{-2}$. Therefore $S_E = 2.4 \times 10^{14} \text{ cm}^{-2} \text{ eV}^{-1}$.

After an oxygen adsorption of 450×10^{-6} Torr min: $\mu_{FE} = 88 \text{ cm}^2 \text{ V}^{-1} \text{ sec}^{-1}$, $\Delta P = 1.5 \times 10^{11}$ and this yields $S_E = 6 \times 10^{13} \text{ cm}^{-2} \text{ eV}^{-1}$.

For the degenerated (100) surface, Fermi statistics have to be used and here²⁸:

$$\left| \frac{\mu_{FE}}{\mu} \right| = \frac{1}{1 + S_E/(A \times \Delta P)^{1/5}}; \quad A = 10^3; \\ \left(\frac{\pi}{3} \right)^2 \frac{m^{*3}}{\epsilon_0 h^3 e^4} \approx 10^{56} \text{ eV}^{-5} \text{ cm}^{-8}. \quad (3)$$

Inserting the values for the clean surface: $\mu_{FE} = 165 \text{ cm}^2 \text{ V}^{-1} \text{ sec}^{-1}$, $\Delta P = 2.4 \times 10^{12} \text{ cm}^{-2}$ one obtains $S_E = 5 \times 10^{14} \text{ cm}^{-2} \text{ eV}^{-1}$. At an oxygen pressure of 10^{-5} Torr, $\mu_{FE} = 180 \text{ cm}^2 \text{ V}^{-1} \text{ sec}^{-1}$, $\Delta P = 6 \times 10^{11} \text{ cm}^{-2}$, $S_E = 3 \times 10^{14} \text{ cm}^{-2} \text{ eV}^{-1}$, i.e., a value even higher than that of the clean (111) surface. The hole mobility was always taken as $2000 \text{ cm}^2 \text{ V}^{-1} \text{ sec}^{-1}$; its deviation from this value at the clean surface determines the accuracy of the S_E values quoted here. Considering this limitation, they are in reasonably good agreement with the value $8 \times 10^{13} \text{ cm}^{-2} \text{ eV}^{-1}$ measured by Portnoy and Handler,³⁰ and $2-3 \times 10^{12} \text{ cm}^{-2}$ (for a discrete trap at the edge of the valence band) published by Palmer *et al.*²⁶ More accurate results can only be obtained when the hole mobility at a clean surface has been measured with reasonable accuracy and under satisfactory experimental conditions.

Though our results are not sufficient to determine the density of recombination centers accurately, an estimate on their order of magnitude can be obtained. Assuming the recombination centers to be acceptor-like and near the Fermi level at the surface, the values $c_p = 10^{-6} \text{ cm}^2 \text{ sec}^{-1}$ and $c_n = 10^{-7} \text{ cm}^2 \text{ sec}^{-1}$ for the hole, electron capture probabilities should have the right order of magnitude.³¹ Taking $s = 600 \text{ cm/sec}$ as an average value for the clean (111) surface, one obtains³¹ a density of 10^{14} cm^{-2} for the surface recombination centers. This is

²⁶ D. R. Palmer, S. R. Morrison, and C. E. Dauenbaugh, *Phys. Rev.* **129**, 608 (1963).

²⁷ F. G. Allen (private communication).

²⁸ G. Heiland, *Fortschr. Physik* **9**, 393 (1961).

²⁹ F. G. Allen and G. W. Gobeli, *Phys. Rev.* **127**, 150 (1962).

³⁰ W. Portnoy and P. Handler, Technical Note No. 2, University of Illinois, ASTIA Document No. AD-210-840, 1959 (unpublished).

³¹ A. Many, *J. Phys. Chem. Solids* **8**, 97 (1959).

a very interesting result because it indicates that at the clean surface the densities of surface states and recombination centers differ by a factor, but not by orders of magnitude. The same is true for the real germanium surface.³¹

ACKNOWLEDGMENTS

The author would like to express his sincerest thanks to Dr. S. P. Wolsky, Dr. E. J. Zdanuk, and

Dr. D. Shooter for their help in designing and operating the ultrahigh vacuum system. Professor H. E. Farnsworth's and Professor J. A. Dillon's assistance during the design of the experimental tube was very much appreciated. I am also indebted to J. Silva for supervising the construction of the tube, to L. Rubin for his help with the electronic equipment, and to W. Gowell and J. Gage for all the glass work. R. Leighton's technical assistance was invaluable.

Optical Properties of Aluminum

H. EHRENREICH,* H. R. PHILIPP, AND B. SEGALL

General Electric Research Laboratory, Schenectady, New York

(Received 31 July 1963)

The frequency-dependent complex dielectric constant $\epsilon(\omega) = \epsilon_1 + i\epsilon_2$ and associated functions are derived in the range 0 to 22 eV by application of the Kramers-Kronig relations to existing reflectance data for clean Al surfaces. The results are quantitatively interpreted in terms of intra- and interband transitions as well as plasma oscillations. The decomposition of $\epsilon(\omega)$ into intra- and interband parts given here is seen to be valid in the presence of electron-electron interactions. Due to these interactions the optical effective mass $m_a = 1.5$, deduced from experiment in the free-carrier region, is appreciably larger than that obtained using Segall's band calculations ($m_a \cong 1.15$). The band calculations are extended to higher energies in order to examine the effect of interband transitions for the range of interest. It is found that the only interband transitions which lead to significant structure in $\epsilon_2(\omega)$ are those that occur around W and Σ in the vicinity of K in the Brillouin zone and that these produce a peak near 1.4 eV. These conclusions are in accord with the experimentally determined $\epsilon_2(\omega)$ which exhibits a peak at 1.5 eV and has no further structure at higher energies. The result of a quantitative calculation of the structure in $\epsilon_2(\omega)$ using a fine mesh of points in \mathbf{k} space and an approximate variation of the momentum matrix element with \mathbf{k} is in good agreement with the experimental results with respect to shape but has a magnitude which is somewhat too low. From the known influence of many-electron effects on the intraband contribution to $\epsilon(\omega)$ and a general sum rule, the corresponding effect on interband transitions may be estimated and shown roughly to account for the difference. The derived $\epsilon(\omega)$ indicates the presence of a sharp plasma resonance at $\hbar\omega_p = 15.2$ eV, in excellent agreement with the results of characteristic energy loss experiments. It is shown that this resonance may be interpreted either in terms of electrons characterized by the low-frequency optical mass and screened by the interband dielectric constant at ω_p or, since the f sum has been essentially exhausted, in terms of the exact asymptotic formula for ϵ in which all carriers are unscreened and have the free-electron mass.

I. INTRODUCTION

THE properties of Al have been studied quite extensively during the past few years. This interest has resulted from the fact that it has been possible to observe a number of phenomena yielding direct information about the Fermi surface, including its topology, notably the de Haas-van Alphen effect,¹ the magneto-acoustic effect,² and cyclotron resonance.³ Further, the band structure has been shown to be nearly free electron-

like by a number of independent calculations,⁴⁻⁶ the results of which are all mutually consistent. These calculations have been quite successful in yielding a Fermi surface in quantitative agreement with the experimental results, although the nature of the connectivity of the third band arms has yet to be resolved.^{7,8}

In this paper we shall discuss in terms of the existing information another type of experiment which yields the optical constants. We shall use an approach similar to that previously shown successful in connection with Ag and Cu.⁹ The optical properties principally yield evidence about excited electronic states of the crystals and, in particular, the magnitude of some gaps at

* Present address: The Division of Engineering and Applied Physics, Harvard University, Cambridge, Massachusetts.

¹ E. M. Gunnerson, *Phil. Trans. Roy. Soc. London* **249A**, 229 (1957); M. G. Priestly, *Proceedings of the Seventh International Conference on Low-Temperature Physics* (University of Toronto Press, 1960), p. 230; W. L. Gordon and K. Larson (private communication).

² B. W. Roberts, *Phys. Rev.* **119**, 1889 (1960); G. Kamm and H. V. Bohm, *Phys. Rev.* **131**, 111 (1963).

³ T. W. Moore and F. W. Spong, *Phys. Rev.* **125**, 846 (1962); **126**, 2261(E) (1962).

⁴ V. Heine, *Proc. Roy. Soc. (London)* **A240**, 361 (1957).

⁵ W. A. Harrison, *Phys. Rev.* **118**, 1182 (1960).

⁶ B. Segall, *Phys. Rev.* **124**, 1797 (1961).

⁷ N. W. Ashcroft, *Phys. Rev. Letters* **3**, 202 (1963).

⁸ B. Segall, *Phys. Rev.* **131**, 121 (1963).

⁹ H. Ehrenreich and H. R. Philipp, *Phys. Rev.* **128**, 1622 (1962).